

See discussions, stats, and author profiles for this publication at: <https://www.researchgate.net/publication/265560154>

Methane reforming with carbon dioxide over La-Ni_x-Ce_{1-x} mixed oxide catalysts

Article in INDIAN JOURNAL OF CHEMISTRY- SECTION A · February 2014

CITATIONS

9

READS

178

10 authors, including:



Vikram Sagar

University of Ljubljana

28 PUBLICATIONS 472 CITATIONS

[SEE PROFILE](#)



Sreelatha Nuvula

Indian Institute of Chemical Technology

15 PUBLICATIONS 642 CITATIONS

[SEE PROFILE](#)



Hanmant Gurav

CSIR - National Chemical Laboratory, Pune

9 PUBLICATIONS 363 CITATIONS

[SEE PROFILE](#)



Upendar Kashaboina

CSIR-Indian Institute of Chemical Technology

23 PUBLICATIONS 254 CITATIONS

[SEE PROFILE](#)

Methane reforming with carbon dioxide over $\text{La-Ni}_x\text{-Ce}_{1-x}$ mixed oxide catalysts

T V Sagar^a, N Sreelatha^a, G Hanmant^b, K Upendar^a, N Lingaiah^a, Kamaraju Seetha Rama Rao^a, C V V Satyanarayana^b, I A K Reddy^c & P S Sai Prasad^{a,*}

^aCSIR-Indian Institute of Chemical Technology, Hyderabad 500 007, India

Email: saiprasad@iict.res.in

^bCSIR-National Chemical Laboratory, Pune 411 008, India

^cNational Institute of Technology, Warangal 506 004, India

Received on 31 January 2014; revised and accepted on 20 February 2014

$\text{La-Ni}_x\text{-Ce}_{1-x}$ mixed oxide ($0 \leq x \leq 1$) catalysts have been hydrothermally prepared, characterized by physico-chemical techniques and evaluated for CO_2 reforming of methane. High conversions are achieved for both methane and carbon dioxide over the $\text{LaNi}_{0.6}\text{Ce}_{0.4}\text{O}_3$ catalyst tested under the conditions of $\text{CO}_2/\text{CH}_4/\text{N}_2$ ratio of 80/80/80 (total flow rate = 240 mL/min), space velocity of 28,800 h^{-1} and at a temperature of 800 °C. The H_2/CO ratio in the syngas is stable at 0.93 ± 0.02 . Exchanging Ni with Ce, rather than with La as reported in the literature, appears to be a better option for the improved performance of the catalysts.

Keywords: Catalysts, Carbon dioxide reforming, Dry reforming, Hydrothermal synthesis, Methane reforming, Mixed oxides, Nickel, Lanthanum, Cerium

Global warming has gained the attention of many environmentalists. The rise in the concentration of greenhouse gases (especially methane and carbon dioxide) in the atmosphere necessitates identification of novel techniques for their emission control, in particular the emphasis is on prevention of carbon dioxide emission as this is substantial. Thus, carbon capture and sequestration is being pursued vigorously. The focus is on considering CO_2 as a cheap raw material for chemical synthesis rather than as a pollutant. CO_2 reforming of methane (dry reforming) thus assumes importance as it not only controls the emission of these two global warming gases, but would also help generate important chemicals via Fischer-Tropsch synthesis. The syngas produced during dry reforming can be used for synthesizing value added oxygenated products¹. However, as the reaction is highly endothermic, it is necessary to operate the reactor at high temperatures (700 – 900 °C). This leads to several potential problems such as stability of the catalyst and sintering. The last few years have experienced a renaissance in investigating suitable catalysts for dry reforming. The success of the transformation depends on the efficiency of the catalyst, whose development is very challenging due to the associated coke formation that affects the activity.

Catalyst systems containing Group VIII metals (except Os), in their reduced state, with fine dispersion on suitable supports are effective for this reaction. Noble metals, especially Pt, Pd, Rh, and Ir have been used as catalysts in many earlier reports^{2,3} due to their interesting intrinsic properties like better resistance to coke and sulfur poisoning. On the other hand, nickel has gained much attention as the active element, based on its technical and economic viability in commercial reforming applications⁴. However, nickel based catalysts exhibit a moderate to rapid deactivation due to coke formation and sintering effects⁵, which occur at high temperatures. The particle size of Ni plays an important role in deciding the stability of the catalysts during dry reforming. Smaller particles are more efficient in suppressing coke formation. In this respect, supported catalysts are less advantageous. Confining Ni in well-defined structures such as perovskites, hexaaluminates, spinels and solid solutions is ideal in arriving at its smaller particles. ABO_3 type perovskites oxides, in which A and B are compatible elements have been found to be efficient and thus are extensively studied. In these systems, the A-site accounts for thermal stability and lanthanum is found to be better than the other rare earth species⁶. The B-site decides the catalytic activity for which Ni has been found

suitable. Literature reveals the evaluation of perovskite type mixed oxides, viz., LaNi_{1-x}M_xO₃ (where M = Mg, Cu, Rh, Ru, Co, Fe, Al, etc.)⁷, La_{1-x}M_xNiO₃ (where M = Ce)⁸ and LaNi_xM_{1-x}O₃ (M = Al, Fe)^{9,10}. Moradi *et al.*⁹ reported LaNi_{0.3}Al_{0.7}O₃ to be the best system, stable for more than 170 h, with 98% of methane conversion at 750 °C. In addition, Ni/Mg/Al/Ce¹¹, CoO-MgO¹², LaBO₃¹³ (B = Co, Ni, Fe, Cr) mixed oxides have also been studied for dry reforming of methane. Lima *et al.*¹⁴ prepared La_xCe_{1-x}NiO₃ perovskite catalysts by substitution of La with Ce and reported moderate activity of the catalysts during the dry reforming. Recently, the efficiency of Ni-Ce solid solutions in partial oxidation of methane has been well reported. The application of these solid solutions to dry reforming of methane is rare. Therefore, it is interesting to study the activity of La-Ce-Ni mixed oxides containing Ni-Ce solid solution for dry reforming of methane. In continuation of our earlier study based on the preparation of these mixed oxides by sol-gel method, in this study we have synthesized a series of LaNi_xCe_{1-x}O₃ systems ($x = 0.2, 0.3, 0.4, 0.6, 0.8$) under hydrothermal conditions. The synthesized catalysts were characterized using several physico-chemical techniques and evaluated for dry reforming. The objective is to study the efficacy of hydrothermal method of catalyst preparation on the activity of the catalysts. In addition, the influence of Ce substitution in LaNiO₃ perovskite, the optimum composition of Ce in LaNi_xCe_{1-x}O₃ that offers the best activity and H₂/CO ratio and the stability of the catalyst in the reaction have also been investigated.

Materials and Methods

Preparation of catalysts

The hydrothermal method¹⁰ was adopted for the synthesis of the tri-metallic LaNi_xCe_{1-x}O₃ catalysts with $0 \leq x \leq 1$. Required amounts of La(NO₃)₃.6H₂O (Fluka), Ni(NO₃)₂.6H₂O (SD Fine) and Ce(NO₃)₃.9H₂O (SD Fine) were separately dissolved in known quantities of hot propionic acid. The solutions were stirred under reflux for 24 h. The respective amounts of the nitrate salts used were such that the finished catalysts contained Ni content with $x = 0.2, 0.3, 0.4, 0.6$ and 0.8 . Initially, nickel and cerium propionic solutions were mixed together and this mixture was then added rapidly to the lanthanum solution. The resulting mixture was hydrothermally treated at 150 °C for 24 h to produce a resin-like material. The resin thus obtained was dried under

reduced pressure and calcined at 800 °C with a temperature ramp of 2 °C/min. Besides, a sample with $x = 1.0$ was also prepared for the sake of comparison.

Characterization of catalysts

The X-ray diffraction patterns of the calcined catalysts were obtained on an Ultima-IV X-ray diffractometer (Rigaku Corporation, Japan) using nickel-filtered Cu K α radiation ($\lambda = 1.54 \text{ \AA}$). The measurements were recorded in steps of 0.045° with count time of 0.5 s in 2 θ range of 10–80°. The crystalline phases were identified with the help of JCPDS files. The specific surface areas of the samples were determined by applying BET method to the N₂ adsorption data obtained at –196 °C using a Smart Sorb 92/93 instrument (SMART Instruments, India). Prior to BET measurement, the samples were dried at 150 °C for 2 h. Temperature programmed reduction (TPR) studies of all the catalysts were performed using a home-made apparatus. Catalysts (50 mg) taken in a quartz reactor were reduced with 10% H₂/Ar gas mixture at a flow rate of 5 °C/min up to 900 °C. Before the TPR run, the catalysts were pretreated in argon at 300 °C for 2 h. The H₂ consumption was monitored on a TCD attached to a Varian gas chromatograph. Fourier transform infrared spectroscopic (FT-IR) studies of catalysts were executed on a Perkin Elmer FT-IR system (Spectrum GX Instrument, USA) using KBr pellet catalysts. XPS measurements were made on a Kratos Axis 165 instrument. The non-monochromatized Al-K α X-ray source ($h\nu = 1486.6 \text{ eV}$) was operated at 12.5 kV and 16 mA. Before acquisition of the data the sample was out-gassed for about 3 h at 100 °C under a pressure of 1.0×10^{-2} torr to minimize surface contamination. The XPS instrument was calibrated using Au as a standard material. For energy calibration, the carbon 1s photoelectron line was used. The carbon 1s binding energy was taken as 285 eV. Charge neutralization of 2 eV was used to balance the charge up of the sample. The spectra were de-convoluted using Sun Solaris based Vision-2 curve resolver. The location and the full width at half maximum (FWHM) value for the species were first determined using spectrum of the pure sample. The location and FWHM of the products, which were not obtained as pure species were adjusted until the best fit was obtained. Symmetric Gaussian shapes were used in all the cases. Binding energies for identical samples were, in general reproducible within $\pm 0.1 \text{ eV}$.

Catalytic activity

The activity of the catalysts was evaluated in a fixed-bed quartz micro reactor (i.d.:12 mm) under atmospheric pressure using a reaction mixture of CO_2 , CH_4 and N_2 continuously at a ratio $\text{CO}_2/\text{CH}_4/\text{N}_2 = 80/80/80$ (total flow rate = 240 mL/min, GHSV of 28,800 h^{-1}). 0.5 cm^3 (0.8 g) of catalyst (18/25 BSS mesh) diluted with ceramic beads of the same size and constituting 50% of the volume of the catalyst. Before starting the reaction, the samples were reduced *in situ* under 60% H_2/N_2 gas at 600 °C for 6 h. The product was analyzed online on a Chemito 8610 gas chromatograph equipped with a carbosphere column using argon as a carrier gas and a TCD detector.

Results and Discussion

Surface area and XRD studies

Table 1 illustrates the change in specific surface area of the catalysts with change in the value of x . It can be seen that the surface area gradually increases with increase in nickel content from $x = 0.2$ – 0.8 as also reported in the literature¹⁵. The X-ray diffraction patterns of the $\text{La-Ni}_x\text{-Ce}_{1-x}$ mixed oxides are displayed in Fig. 1, including that of LaNiO_3 perovskite. The peaks at 23.6, 32.9, 47.3 and 58.9° (2 θ) are in agreement with the characteristic lines of the rhombohedral phase of LaNiO_3 (JCPDF 34-1028). The intensity of these peaks is higher as the x value reaches 0.8 and 1.0 than the catalysts with lower x values. At low x values peaks due to La_2O_3 (2 θ = 27.5, 31.2, 45.8 and 54.3°) dominate. A shift in the 2 θ values towards lower angles is evidenced with increasing x . This is due to the dissolution of Ni^{2+} ions in the La_2O_3 lattice forming the LaNiO_3 perovskite, as seen in catalysts with higher values of x . A drastic decrease in the surface area in these samples with high x values also indicates the formation of crystalline perovskite. The NiO shows highly diffused peaks in catalysts with low Ni content, probably due to the presence of smaller particles which are not being detected by XRD. This indicates the presence of

highly dispersed Ni particles supported on La_2O_3 or CeO_2 . However, their presence is visualized in catalysts with high x values. Interestingly, peaks due to crystalline CeO_2 are not observed. With the substitution of La by Ce, Lima *et al.*¹⁴ reported the formation of discrete crystalline phase of CeO_2 , in addition to LaNiO_3 . On the other hand, in the present work when Ce was substituted for Ni, CeO_2 becomes amorphous and La_2O_3 is crystallized out. There is also the possibility of the formation of Ce-Ni solid solution at low values of x , as reported in the literature¹⁴, though it is not clearly visible in the XRD patterns of the present catalysts. It is also reported that nickel exists in two phases in the Ce-Ni systems Ni as NiO on the surface of the ceria and Ni^{2+} ions incorporated in the CeO_2 lattice^{15,16}.

TPR studies

Figure 2 provides the TPR patterns of the $\text{LaNi}_x\text{Ce}_{1-x}$ oxide catalysts. LaNiO_3 (inset) exhibits two peaks corresponding to $\text{Ni}^{3+} \rightarrow \text{Ni}^{2+}$ and $\text{Ni}^{2+} \rightarrow \text{Ni}^0$ reduction with the area ratio of second/first equaling 2, as reported in the literature¹⁷. The peak shapes and their temperature maxima are found to vary with change in Ni composition. As revealed by the XRD patterns, at low x values, the catalysts essentially contain La_2O_3 as a discrete phase, which is not easily reducible. Ni and Ce oxides which are alone or in the mixed form are reducible. Yonggang *et al.*¹⁷ divided the TPR peaks into α , β , γ

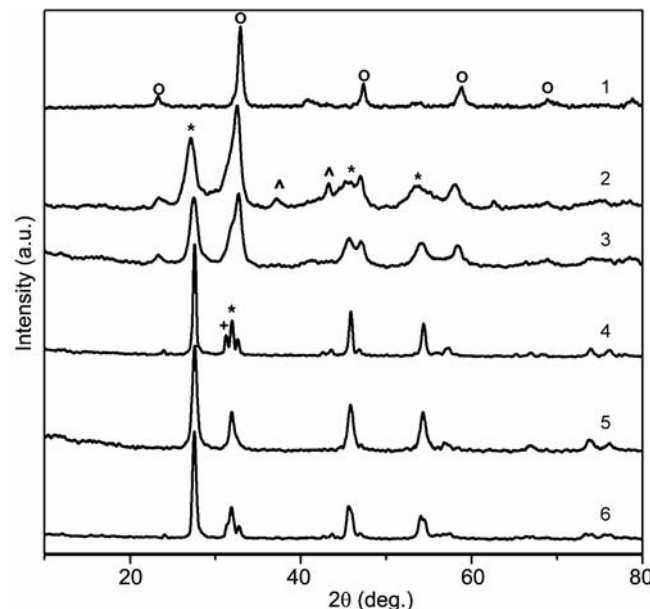


Fig. 1 – XRD patterns of $\text{La-Ni}_x\text{-Ce}_{1-x}$ mixed oxide. [1, $x = 1$; 2, $x = 0.8$; 3, $x = 0.6$; 4, $x = 0.4$; 5, $x = 0.3$; 6, $x = 0.2$. (*) La_2O_3 , (O) LaNiO_3 , (•) CeO_2 , (+) La_2NiO_4 , (^) NiO_2].

Table 1 – Specific surface area (SSA) and IR band frequencies of $\text{La-Ni}_x\text{-Ce}_{1-x}$ mixed oxide systems

Catalyst	SSA (m^2/g)	IR (cm^{-1})	
		(N-O)	M-O
$\text{LaNi}_{0.8}\text{Ce}_{0.2}\text{O}_3$	4.1	1372	528
$\text{LaNi}_{0.6}\text{Ce}_{0.4}\text{O}_3$	3.9	1369	489
$\text{LaNi}_{0.4}\text{Ce}_{0.6}\text{O}_3$	3.5	1380	529
$\text{LaNi}_{0.3}\text{Ce}_{0.7}\text{O}_3$	2.2	1381	532
$\text{LaNi}_{0.2}\text{Ce}_{0.8}\text{O}_3$	0.4	1386	546

and δ types in the case of Ni containing CeO₂ catalysts. The α peak arising at around 330 °C is due to the reduction of the adsorbed oxygen on the Ni-Ce mixed oxide. The β appearing at 400 °C represents the reduction of NiO particles dispersed on ceria and the γ , normally seen at around 550 °C, to the reduction of NiO intimately in contact with CeO₂. The δ peak, on the other hand, represents the reduction of CeO₂ with its characteristic peak displayed beyond

800 °C (not seen in the present patterns). It is evident from the TPR profile that the areas of both β and γ peaks are enhanced with increasing nickel content, particularly the peak at higher temperatures (γ). This is in agreement with the fact that CeO₂ influences the reduction of the Ni species to metallic nickel. On the other hand, the merging of γ with β implies agglomeration of NiO. The appearance of distinct peaks due to NiO in the XRD patterns of the catalysts with $x = 0.6$ and 0.8 lends credence to this phenomenon. At lower Ni compositions there is the possibility of the formation of a nickel oxide-ceria solid solution¹⁴. However, the reducibility of Ni species in the solid solution is difficult. The TPR peak with its maximum appearing at 500–600 °C could be due to the Ni in solid solution. Thus, in support of the XRD results, the TPR information also confirms the presence of the perovskite (LaNiO₃) in the catalysts with high Ni loading and the existence of NiO in two forms, i.e., the interacted (with CeO₂) and the well dispersed species. Particularly, the catalyst with $x = 0.4$ displays the presence of both forms.

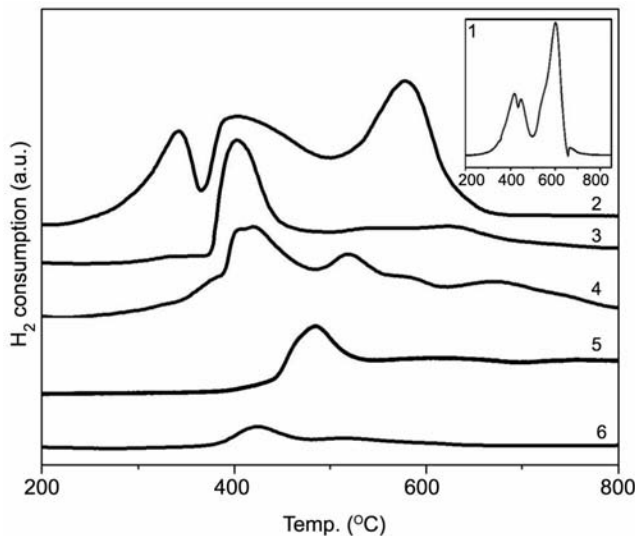


Fig. 2 – TPR patterns of LaNi_xCe_{1-x}O₃ perovskite type. [1, $x = 1$; 2, $x = 0.8$; 3, $x = 0.6$; 4, $x = 0.4$; 5, $x = 0.3$; 6, $x = 0.2$].

X-ray photoelectron spectroscopy

The core level binding energies of the Ce 3d, La 3d, Ni 2p, C 1s and O 1s of La-Ni_x-Ce_{1-x} mixed oxides are shown in Fig. 3. Due to the closeness of the binding energies of Ni 2p_{3/2} and La 3d_{5/2}, it is difficult

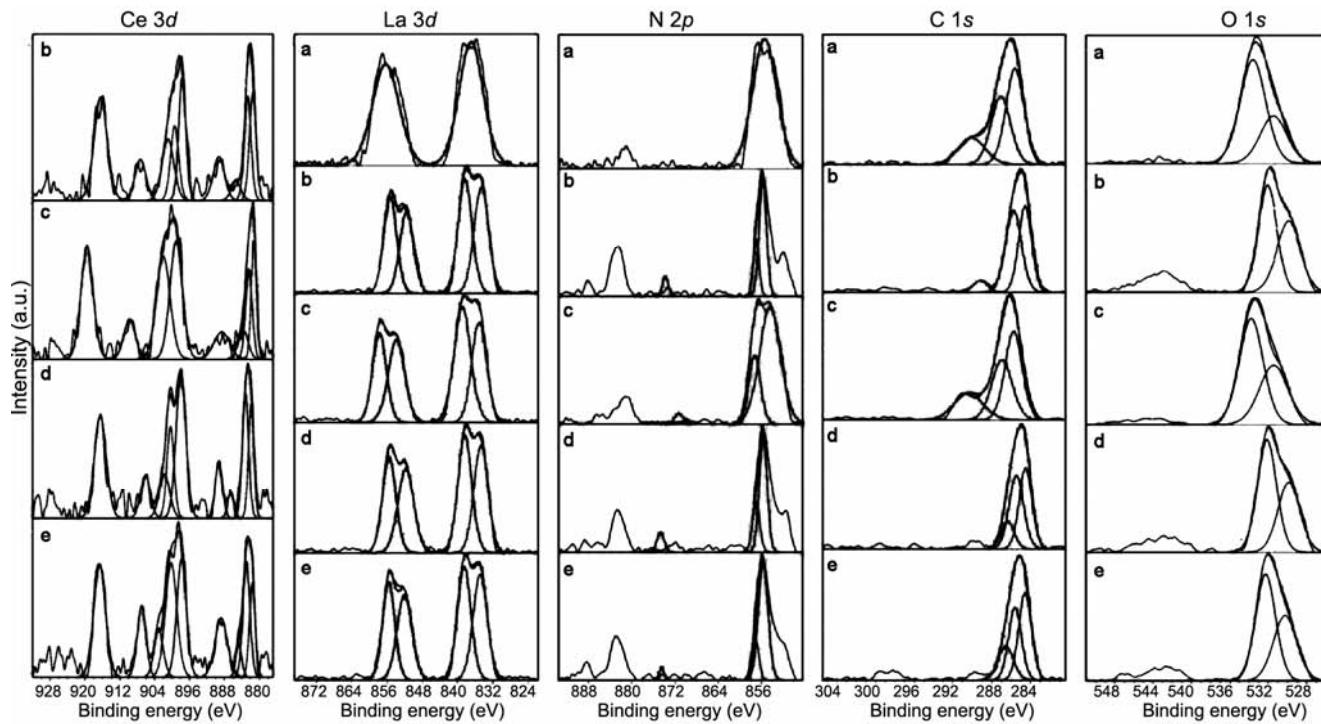


Fig. 3 – Core level spectra of La-Ni_x-Ce_{1-x} mixed oxide catalysts. [(a) $x = 1$; (b) $x = 0.6$; (c) $x = 0.4$; (d) $x = 0.3$; (e) $x = 0.2$].

to distinguish between these two species¹⁸. However, the binding energies recorded at 855.3 and 838.3 eV fit well with La $3d_{3/2}$ and $3d_{5/2}$ states, respectively. The most intense 855.3 eV peak overlaps with that of the Ni $2p$ peak due to Ni²⁺ in NiO. Figure 3 also shows the Ce $3d$ profiles of the catalyst samples. The binding energies of the $3d_{5/2}$ are more intense suggesting that cerium exists in Ce⁴⁺ oxidation state. These results support the observations of TPR and XRD characterization where the Ce-Ni interaction prevails in the low Ni containing catalysts. In the O 1s spectra, the peaks appearing between 529.2–531.9 eV and 529.9–532.3 eV arise from hydroxyl and carbonate groups and adsorbed water¹⁹. The C 1s shows peaks at 284.6 and 285.9 eV which may be due to hydrocarbon contamination (C-C/C-H and C-O bonds). Besides, the small peak observed with binding energy in the region of 288.9–289.3 eV represents the carbonate species^{19,20} which reacts with La³⁺ when exposed to atmosphere.

FT-IR and morphology

FT-IR spectra of catalysts are shown in Fig. 4. Since nitrate precursors are used in catalyst preparation it is expected that residual nitrates are present on the coordination sphere of the corresponding metallic cation, which in turn is surrounded by a propionic acid molecule (bands \sim 1369 and \sim 1472 cm⁻¹). The frequencies around \sim 3000–3600 cm⁻¹ correspond to –OH stretching of structural hydroxyl groups and physisorbed and interlayer water¹¹. The IR spectrum of LaNiO₃ catalyst does not show any characteristic peak due to

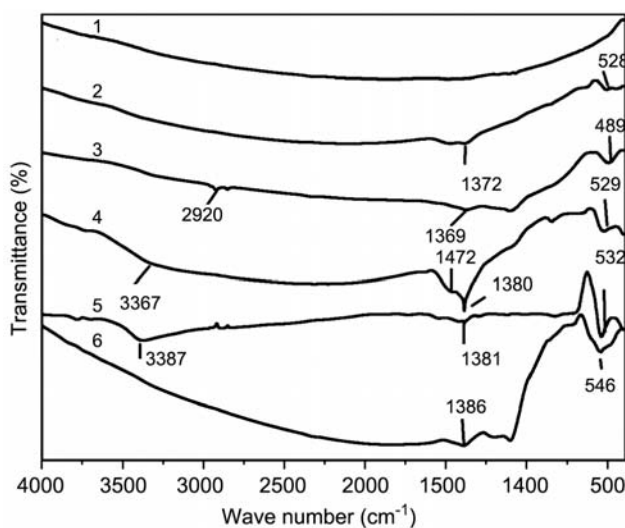


Fig. 4 – IR spectra of $\text{LaNi}_x\text{Ce}_{1-x}\text{O}_3$ perovskite catalysts. [1, $x = 1$; 2, $x = 0.8$; 3, $x = 0.6$; 4, $x = 0.4$; 5, $x = 0.3$; 6, $x = 0.2$].

its low resistivity^{21,22}. The catalysts with $x = 0.2, 0.3, 0.4, 0.6$ and 0.8 show bands in the region 546–489 cm⁻¹, which are in agreement with the vibrational stretching frequencies of the metal-oxygen bonds²³. The nitrate peak in the region of 830 cm⁻¹ is often restricted in the propionic acid mediated synthesis of perovskites⁹.

Catalytic activity

The catalytic functionalities of the hydrothermally synthesized catalysts obtained at 800 °C are displayed in Fig. 5. There is almost a linear increase in the activity of the catalyst initially from $x = 0.2$ to 0.4 , then it remains steady up to 0.6 and then on there is a sudden drop at $x = 0.8$. With increasing composition of Ni, initially there is an increasing dispersion of NiO on La₂O₃ or on the Ce-Ni solid solution, thereby increasing the catalytic activity. CeO₂ promotes the activation of CO₂ due to its redox property ($\text{Ce}_2\text{O}_3 + \text{CO}_2 = 2\text{CeO}_2 + \text{CO}$). La₂O₃, being basic, could have provided the necessary sites for the adsorption of CO₂. Higher composition of Ni primarily helped in LaNiO₃ formation, which is not as active as the dispersed Ni oxide. The depletion of free La₂O₃ also decreases the CO₂ adsorption capacity. Hence, there is a sudden drop in the catalytic activity. Among all the catalysts screened, LaNi_{0.6}Ce_{0.4}O₃ is found to exhibit the highest activity in terms of CH₄ (94%) and CO₂ (96%) conversions and H₂/CO ratio (0.94) as compared to that of the catalysts reported by Lima *et al.*¹⁴, with 53% and 62% conversion of CH₄ and CO₂ respectively.

The results of time-on-stream analysis performed on LaNi_{0.6}Ce_{0.4}O₃ catalyst at 800 °C are plotted in Fig. 6. The catalyst could retain its

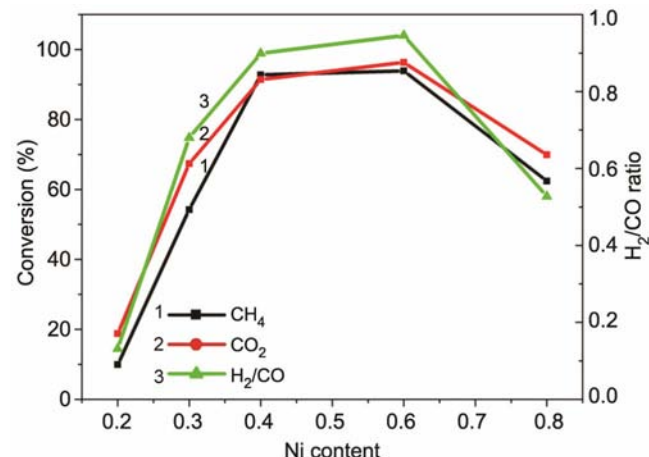


Fig. 5 – Activity profiles of $\text{LaNi}_x\text{Ce}_{1-x}\text{O}_3$ catalysts at 800 °C. [1, CH₄; 2, CO₂; 3, H₂/CO].

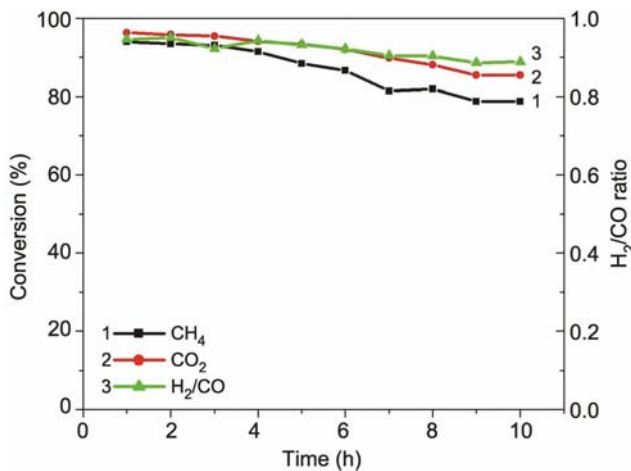


Fig. 6 – Time-on-stream analysis of LaNi_{0.6}Ce_{0.4}O₃ catalyst. [1, CH₄; 2, CO₂; 3, H₂/CO].

activity to a larger extent during the period of evaluation showing a reasonable stability. The presence of the Ni species with strong interaction with CeO₂ helps in resisting coke formation. Similarly, the syngas ratio is also retained in the region of 0.94–0.88. The H₂/CO ratio of the product gas in dry reforming is always less than the stoichiometric ratio of 1:1 as this reaction is always accompanied by the reverse water gas reaction.

Conclusions

The hydrothermally synthesized catalysts are substantially more active than the perovskites reported in the literature. LaNi_{0.6}Ce_{0.4}O₃ is the optimum composition for the catalyst. The catalyst also shows better stability in terms of CH₄ and CO₂ conversions as well as the H₂/CO ratio.

Acknowledgement

The authors thank Department of Science and Technology, New Delhi, India, and, Council for Scientific and Industrial Research, New Delhi, India

for the financial support under DST/IS-STAC/CO2-SR-146/12 (G) and NWP-0021 projects, respectively.

References

- 1 Burch R & Petch M I, *Appl Catal A*, 88 (1992) 39.
- 2 Solymosi F, Kutsan G & Erdöhelyi A, *Catal Lett*, 11 (1991) 149.
- 3 Torniainen P M, Chu X & Schmidt L D, *J Catal*, 146 (1994) 1.
- 4 Tsang S C, Claridge J B & Green M L H, *Catal Today*, 23 (1995) 3.
- 5 Rostrup-Nielsen J R, in *Catal Sci Technol*, Vol. 5, edited by J R Anderson & M Boudart, (Springer, Berlin) 1984, pp. 1-117.
- 6 Mawdsley J R & Krause T R, *Appl Catal A*, 334 (2008) 311.
- 7 Moradi G R, Khosravian F & Rahmanzadeh M, *Chinese J Catal*, 33 (2012) 797.
- 8 Qi A, Wang S, Fu G, Ni C & Wu D, *Appl Catal A*, 281 (2005) 233.
- 9 Moradi P & Parvari M, *Iran J Chem Eng*, 3 (2006) 29.
- 10 Provendier H, Petit C, Schmitt J L, Kienneman A & Chaumont C, *J Mater Sci*, 34 (1999) 4121.
- 11 Daza C E, Gallego J, Moreno J A, Mondragón F, Moreno S & Molina R, *Catal Today*, 133-135 (2008) 357.
- 12 Choudhary V R, Mondal K C & Choudhary T V, *Ind Eng Chem Res*, 45 (2006) 4597.
- 13 Wu Y, Kawaguchi O & Matsuda T, *Bull. Chem. Soc. Japan*, 71 (1998) 563.
- 14 Lima S M, Assaf J M, Peña M A & Fierro J L G, *Appl Catal A*, 311 (2006) 94.
- 15 Sohier M P, Wrobel G & Bonnelle J P, *Appl Catal A*, 84 (1992) 169.
- 16 Lamonier C, Ponchel A, Huysser A D & Jalowiecki-Duhamel L, *Catal Today*, 50 (1999) 247.
- 17 Yonggang W, Hua W, Kongzhai L, Xing Z & Yunpeng D, *J Rare Earth*, 28 (2010) 357.
- 18 Haack L P, Peters C R, Vriesand J E & Otto K, *Appl Catal A*, 87 (1992) 103.
- 19 Fierro J L G, *Catal Today*, 8 (1990) 153.
- 20 Peña M A & Fierro J L G, *Chem Rev*, 101 (2001) 1981.
- 21 Ganguly P & Vasanthacharya N Y, *J Solid State Chem*, 61 (1986) 164.
- 22 Vaz T & Salker A V, *Mater Sci Eng B*, 143 (2007) 81.
- 23 *The Handbook of Infrared and Raman Spectra of Inorganic Compounds and Organic Salts*, Vol. 4, edited by R A Nyquist, C L Putzig & M A Leugers, (Academic Press Ltd., San Diego, CA) 1997.